Journal of Computational and Applied Mathematics 359 (2019) 102–118

Contents lists available at ScienceDirect

Journal of Computational and Applied Mathematics

journal homepage: www.elsevier.com/locate/cam

Discrete approximation for a two-parameter singularly perturbed boundary value problem having discontinuity in convection coefficient and source term

T. Prabha [a], M. Chandru [b], V. Shanthi [a], H. Ramos [c,d,*]

[a] Department of Mathematics, National Institute of Technology, Tiruchirappalli 620 015, Tamilnadu, India
[b] Department of Sciences and Humanities, Division of Mathematics, Vignan's Foundation for Science Technology & Research, Guntur 522 216, Andhra Pradesh, India
[c] Scientific Computing Group, Universidad de Salamanca, Spain
[d] Escuela Politécnica Superior, Campus Viriato, 49022, Zamora, Spain

ARTICLE INFO

Article history:
Received 24 July 2018
Received in revised form 9 March 2019

Keywords:
Singularly perturbed problem
Boundary and interior layers
Two small parameters
Shishkin mesh
Finite difference scheme
Convergence analysis

ABSTRACT

In this study we present a method for approximating the solution of a Singularly Perturbed Boundary Value Problem (SPBVP) containing two parameters $(\varepsilon_1, \varepsilon_2)$, which multiply the diffusion coefficient and the convection term, respectively. Moreover, we consider that the convection coefficient and the source term present a discontinuity at an intermediate point. Theoretical bounds for the solution and its derivatives are derived for two complementary cases. A parameter uniform numerical scheme is constructed, which involves an upwind finite difference method with an appropriate piecewise uniform mesh. The error estimation and convergence analysis are presented, which show that the scheme provides a parameter uniform convergence of almost first order. Some numerical examples are discussed to illustrate the performance of the present method.

1. Introduction

The theory of Singularly Perturbed Problems (SPPs) has been developed for over a century. Consistently, such problems are expressed as differential equations which contain at least one small parameter multiplying the highest derivative term. These kind of SPPs arise in various fields such as fluid dynamics, mechanics, transport phenomena in biology and chemistry, semi-conductor devices, chemical reactor theory and convection–diffusion processes.

The solutions to SPPs depend on the presence of a small, positive parameter that varies very rapidly in some parts of the region of integration subject to the presence of boundary or interior layer(s), and varies slowly in other parts. The primary signet of a singular perturbation problem is that a simple and straightforward approximation does not give an accurate solution throughout the domain of that solution. The numerical treatment of SPPs is accompanied by significant computational difficulties due to the presence of sharp layers in the solution. Therefore, more efficient and underlying computational methods are required to overcome the issues. Despite a tremendous amount of work being done in this research field of SPPs, there is still a platform for more relevant research to explore. A great number of special purpose methods were developed by the researchers to provide rigorous numerical solutions, which focus second order differential equations with single parameter for continuous data [1–5] and also for discontinuous data [6–9].

* Corresponding author at: Escuela Politécnica Superior, Campus Viriato, 49022, Zamora, Spain.
E-mail addresses: prabha.thevaraj@gmail.com (T. Prabha), leochandru@gmail.com (M. Chandru), vshanthi@nitt.edu (V. Shanthi), higra@usal.es (H. Ramos).

https://doi.org/10.1016/j.cam.2019.03.040
0377-0427/

All the works mentioned above are concerned to SPPs in which a small parameter perturbs the highest derivative term. But we might encounter problems involving more than one parameter. Two-parameter problems have not been studied so extensively like single parameter problems. For the first time, a two-parameter SPP was analyzed by O'Malley [10]. He discussed the asymptotic behavior of the solution when the two parameters ε_1 and ε_2 tend to zero. The solution is influenced by the order of $\varepsilon_1/\varepsilon_2^2$ and $\varepsilon_2^2/\varepsilon_1$. Vigo et al. in [11] considered a non-overlapping domain decomposition method in order to approximate the solution of a two-parameter SPP.

A few researchers have considered the convection–reaction–diffusion problem with continuous data. For instance, Roos and Uzelac [12] developed a second order parameter uniform method for the two-parameter problem using streamline diffusion finite element method. A non-standard finite difference method for two-parameter SPPs was developed in [13]. Shishkin [14] considered an exponentially fitted difference scheme on an equidistant mesh with order of convergence $CN^{-2/5}$. O'Riordan et al. discussed a first order parameter uniform numerical algorithm based on upwind finite difference operator [15]. Two-parameter SPPs with non-smooth data is an open research area to explore. Shanthi et al. [16] considered a convection–reaction–diffusion problem with discontinuity in the source term. A similar type of problem was considered in [17]. Falco and Riordan [18] constructed and analyzed the SPP with non-smooth data that is similar to the two-parameter problem. Also, the authors have discussed with an example that these type of problems arise in the modeling of phase transitions. The articles [15,16] motivated the present study concerning a two-parameter SPP in one-dimension with discontinuous source and convection coefficient of the form:

$$\mathcal{L}y(x) \equiv \varepsilon_1 y''(x) + \varepsilon_2 a(x)y'(x) - b(x)y(x) = f(x), \quad \forall\, x \in (\Omega^- \cup \Omega^+), \tag{1.1}$$

$$y(0) = y_0, \qquad y(1) = y_1, \tag{1.2}$$

$$a(x) \le -\alpha_1 < 0 \text{ for } x \in \Omega^- \quad \text{and} \quad a(x) \ge \alpha_2 > 0, \quad \text{for } x \in \Omega^+, \tag{1.3}$$

$$|\,[a](d)\,| \le C, \qquad |\,[f](d)\,| \le C. \tag{1.4}$$

It is conducive to introduce the representation $\overline{\Omega} = [0, 1]$, $\Omega^- = (0, d)$ and $\Omega^+ = (d, 1)$. We assume that $b(x) \ge \gamma > 0$ is a sufficiently smooth function in $\overline{\Omega}$, and $a(x), f(x)$ are sufficiently smooth functions in $(\Omega^- \cup \Omega^+) \cup \{0, 1\}$. Also $a(x), f(x)$ and their derivatives have a jump discontinuity at $d \in \Omega = (0, 1)$, denoted by $[w](d) = w(d+) - w(d-)$ and $0 < \varepsilon_1 \ll 1$, $0 \le \varepsilon_2 < 1$.

With the above assumptions, the SPP (1.1)–(1.4) has a solution $y(x) \in C^0(\overline{\Omega}) \cap C^1(\Omega) \cap C^2(\Omega^- \cup \Omega^+)$. So far, the SPP (1.1)–(1.4) has not been considered by any author, due to the complexity of the solution. Hence it is interesting to study the behavior of this type of problem and moreover, when $\varepsilon_2 = 1$, the above problem behaves like the convection–diffusion problem in [9], and when $\varepsilon_2 = 0$ it behaves like the well known reaction–diffusion problem in [6]. In what follows two separate cases are considered :

Case (i): $\sqrt{\alpha}\varepsilon_2 \le \sqrt{\rho\varepsilon_1}$ and **Case (ii):** $\sqrt{\alpha}\varepsilon_2 > \sqrt{\rho\varepsilon_1}$ where $\rho = \min\limits_{x \in \overline{\Omega}\setminus\{d\}} \left\{ \left| \dfrac{b(x)}{a(x)} \right| \right\}$ and $\alpha = |\min\{\alpha_1, \alpha_2\}|$.

All through this paper $C > 0$ represents a constant independent of the mesh length (N) and the perturbation parameters (ε_1, ε_2). The norm considered is the supremum norm, denoted by

$$\|z\|_{\overline{\Omega}} = \sup_{x \in \overline{\Omega}} |z(x)|.$$

The rest of the paper is organized as follows. In Section 2 some *a priori* results are described for the continuous problem. Discretization of the continuous problem and the methods to be applied with the discrete bounds are described in Section 3. Decomposition and bounds for the discrete solution are presented in Section 4. In Section 5 the convergence of the numerical method is analyzed, resulting that an almost first order accuracy, consistent with the parameters $(\varepsilon_1 - \varepsilon_2)$ is obtained. Some numerical illustrations are presented in Section 6 to show the performance of the proposed method. The paper ends with a conclusion.

Note. If the discontinuity assumed in the convection coefficient is reversed (to that defined in this manuscript) like $a(x) \ge \alpha_1 > 0$, $x \in \Omega^-$, and $a(x) \le -\alpha_2 < 0$, $x \in \Omega^+$, the change noticed is remarked in the error estimates.

2. A priori bounds on the solution and its decomposition

In this section, analytical properties, the existence of the solution, minimum principle, uniform stability and bounds for the derivatives of the solution of the problem in (1.1)–(1.4) and how to decompose the solution are discussed.

Theorem 2.1. *The SPP (1.1)–(1.4) has a solution $y(x) \in C^0(\overline{\Omega}) \cap C^1(\Omega) \cap C^2(\Omega^- \cup \Omega^+)$.*

Proof. Following the methods presented in [15,19] a solution of the SPP (1.1)–(1.4) can be easily obtained. □

For the continuous problem in (1.1)–(1.4) the operator $\mathcal{L}$ satisfies the following minimum principle on $\overline{\Omega}$.

Lemma 2.2. *Suppose that a function $z(x) \in C^0(\overline{\Omega}) \cap C^2(\Omega^- \cup \Omega^+)$ satisfies $z(0) \ge 0$, $z(1) \ge 0$, and $\mathcal{L}z(x) \le 0$, $x \in (\Omega^- \cup \Omega^+)$ and $[z'](d) \le 0$. Then $z(x) \ge 0$, $\forall\, x \in \overline{\Omega}$.*

Proof. Let $\tilde{x}$ be any point at which $z(x)$ reaches its minimum value in $\overline{\Omega}$. If $z(\tilde{x}) \geq 0$, then the result is evident. Suppose that $z(\tilde{x}) < 0$, with the boundary values assumed, either $\tilde{x} \in (\Omega^- \cup \Omega^+)$ or $\tilde{x} = d$. Consider $\tilde{x} \in (\Omega^- \cup \Omega^+)$. Now $z'(\tilde{x}) = 0,\ z''(\tilde{x}) \geq 0$. Hence

$$\mathcal{L}z(\tilde{x}) = \varepsilon_1 z''(\tilde{x}) + \varepsilon_2 a(\tilde{x}) z'(\tilde{x}) - b(\tilde{x}) z(\tilde{x}) > 0,$$

which is a contradiction. Here $a(x)$ is defined as (1.3). The only possibility is to choose $\tilde{x} = d$. The argument depends on the differentiability of $z(x)$ at d. Though $z''(x)$ has a discontinuity at d, it is a smooth function on the interval $N_h = (d, d+\delta]$. If $z'(\tilde{x})$ does not exist then $z'(x) \geq 0$ in the neighborhood $(d, d+\delta)$, $\delta \geq 0$. Applying the fundamental theorem of calculus we have $z'(x) = \int_{d+0}^{x} z''(s)ds$ with $z''(x) \geq 0$, $x \in N_h$. Hence for $x \in N_h$ it is $\mathcal{L}z(x) > 0$, which is a contradiction to our assumption. Therefore $z(x) \geq 0$ for all $x \in \overline{\Omega}$. □

An immediate consequence of the minimum principle is the next lemma. Lemmas 2.3 and 2.4 can be proved using the principles adopted in [15].

Lemma 2.3. *Let $y(x)$ be a solution of (1.1)–(1.2), then*

$$\|y\|_{\overline{\Omega}} \leq \max\{|y(0)|,\ |y(1)|\} + \frac{1}{\gamma}\|f\|_{(\Omega^- \cup \Omega^+)}.$$

Lemma 2.4. *Let $y(x)$ be the solution of the problem (1.1)–(1.2) where $|y(0)| \leq C,\ |y(1)| \leq C$. Then, for $k = 1, 2, 3$, it holds that*

$$\|y^{(k)}\|_{\overline{\Omega}} \leq \frac{C}{\left(\sqrt{\varepsilon}_1\right)^k}\left(1 + \left(\frac{\varepsilon_2}{\sqrt{\varepsilon}_1}\right)^k\right) \max_{x \in \overline{\Omega}}\{\|y\|, \|f\|\}, \quad k = 1, 2,$$

$$\|y^{(3)}\|_{\overline{\Omega}} \leq \frac{C}{\left(\sqrt{\varepsilon}_1\right)^3}\left(1 + \left(\frac{\varepsilon_2}{\sqrt{\varepsilon}_1}\right)^3\right) \max_{x \in \overline{\Omega}}\left\{\|y\|, \|f\|, \|f'\|\right\}.$$

2.5. Decomposition of the solution

Consider the following perceptions before decomposing $y(x)$. Let $G(x)$ be any smooth function in $(\Omega^- \cup \Omega^+)$ with a jump discontinuity at $d \in D$. Suppose our goal is to find a function $u(x) \in C^1(\Omega) \cap C^2(\Omega^- \cup \Omega^+)$ such that

$$\begin{cases} \mathcal{L}u = G(x), & x \in \Omega^- \cup \Omega^+, \\ u(0) = q_1, \quad u(1) = q_2. \end{cases} \tag{2.1}$$

The problem in (2.1) has a unique solution (see [19]). Let

$$G_l^{(k)*}(x) = \begin{cases} G^{(k)}(x), & x \in (0, d) \\ G^{(k)}(d-) & \text{at} \quad x = d \end{cases}$$

and

$$G_r^{(k)*}(x) = \begin{cases} G^{(k)}(d+) & \text{at} \quad x = d \\ G^{(k)}(x), & x \in (d, 1) \end{cases}$$

where $G^{(k)}$ stands for the k^{th} derivative of G. Now, define

$$\begin{cases} \mathcal{L}u_l^* = G_l^*(x), & x \in (0, d), \\ u_l^*(0) = q_1, \quad u_l^*(d) = y(d), \end{cases} \tag{2.2}$$

and

$$\begin{cases} \mathcal{L}u_r^* = G_r^*(x), & x \in (d, 1), \\ u_r^*(d) = y(d), \quad u_r^*(1) = q_2. \end{cases} \tag{2.3}$$

It can be easily established that

$$u(x) = \begin{cases} u_l^*(x), & x \in [0, d), \\ u_l^*(d) = u_r^*(d), & x = d, \\ u_r^*(x), & x \in (d, 1]. \end{cases}$$

To obtain sharper bounds in the error analysis the solution $y(x)$ is decomposed into regular $v^*(x)$ and singular $w^*(x)$ components. The solution $y(x)$ is decomposed as $y(x) = v^*(x) + w_l^*(x) + w_r^*(x)$ for the two cases. The regular component $v^*(x)$ is the solution of

$$\mathcal{L}v^*(x) = f(x), \quad x \in (\Omega^- \cup \Omega^+), \tag{2.4}$$

$$v^*(0) = y(0),\ v^*(1) = y(1),\ v^*(d-) \text{ and } v^*(d+) \text{ are chosen}, \tag{2.5}$$

where

$$v^*(x) = \begin{cases} v^{*-}(x), & x \in \Omega^-, \\ v^{*+}(x), & x \in \Omega^+. \end{cases}$$

The singular components $w_l^*(x)$ and $w_r^*(x)$ are the solutions of

$$\mathcal{L}w_l^*(x) = 0, \qquad \mathcal{L}w_r^*(x) = 0, \quad x \in (\Omega^- \cup \Omega^+), \tag{2.6}$$

$$w_l^*(0) = y(0) - v^*(0) - w_r^*(0), \qquad w_r^*(1) = y(1) - v^*(1) - w_l^*(1),$$

$$w_l^*(1) \quad \text{and} \quad w_r^*(0), \text{ are chosen suitably,} \tag{2.7}$$

$$[w_r^*](d) = -[v^*](d) - [w_l^*](d) \quad \text{and} \quad [w_r^{*'}](d) = -[v^{*'}](d) - [w_l^{*'}](d), \tag{2.8}$$

where

$$w_l^*(x) = \begin{cases} w_l^{*-}(x), & x \in \Omega^-, \\ w_l^{*+}(x), & x \in \Omega^+, \end{cases} \qquad w_r^*(x) = \begin{cases} w_r^{*-}(x), & x \in \Omega^-, \\ w_r^{*+}(x), & x \in \Omega^+. \end{cases}$$

Note that $v^*(x)$, $w_l^*(x)$ and $w_r^*(x)$ are discontinuous at $x = d$, but by (2.8) their sum is in $\mathcal{C}^1(\Omega)$.

Consider the Case (i): $\sqrt{\alpha}\varepsilon_2 \le \sqrt{\rho\varepsilon_1}$.

Let $v^*(x) = v_0^*(x) + \sqrt{\varepsilon}_1 v_1^*(x) + \varepsilon_1 v_2^*(x)$, where $v_0^*(x)$, $v_1^*(x)$ and $v_2^*(x)$ are the solutions of the following problems respectively:

$$-b(x)v_0^*(x) = f(x), \quad x \in (\Omega^- \cup \Omega^+),$$

$$-b(x)v_1^*(x) = \frac{-\varepsilon_2}{\sqrt{\varepsilon}_1} a(x) v_0^{*'}(x) - \sqrt{\varepsilon}_1 v_0^{*''}(x), \quad x \in (\Omega^- \cup \Omega^+),$$

$$Lv_2^*(x) = \frac{-\varepsilon_2}{\sqrt{\varepsilon}_1} a(x) v_1^{*'}(x) - \sqrt{\varepsilon}_1 v_1^{*''}(x), \quad x \in (\Omega^- \cup \Omega^+),$$

$$v_2^*(0) = v_2^*(1) = 0, \ v_2^*(d-), \ v_2^*(d+) \text{ are chosen,}$$

where $v_2^* \in \mathcal{C}^0(\overline{\Omega}) \cap \mathcal{C}^1(\Omega) \cap \mathcal{C}^2(\Omega^- \cup \Omega^+)$. Lemmas 2.6 and 2.7 can be proved following the principles and methods adopted in [2,15].

Lemma 2.6. *The regular component $v^*(x)$ satisfies the following bound*

$$\|v^{*(k)}\|_{\Omega\setminus\{d\}} \le C\left(1 + \frac{1}{(\sqrt{\varepsilon}_1)^{k-2}}\right), \quad \text{for } k = 0, 1, 2, 3.$$

Lemma 2.7. *The singular components $w_l^*(x)$ and $w_r^*(x)$ satisfy the following bounds*

$$\|w_l^{*(k)}\|_{\Omega\setminus\{d\}} \le \frac{C}{(\sqrt{\varepsilon}_1)^k} \begin{cases} Ce^{-\theta_2 x}, & x \in \Omega^-, \\ Ce^{-\theta_1(x-d)}, & x \in \Omega^+, \end{cases} \quad k = 0, 1, 2 \text{ and } 3,$$

$$\|w_r^{*(k)}\|_{\Omega\setminus\{d\}} \le \frac{C}{(\sqrt{\varepsilon}_1)^k} \begin{cases} Ce^{-\theta_1(d-x)}, & x \in \Omega^-, \\ Ce^{-\theta_2(1-x)}, & x \in \Omega^+, \end{cases} \quad k = 0, 1, 2 \text{ and } 3,$$

where

$$\theta_1 = \begin{cases} \dfrac{\sqrt{\rho\alpha}}{\sqrt{\varepsilon}_1}, & \text{if } \sqrt{\alpha}\varepsilon_2 \le \sqrt{\rho\varepsilon_1}, \\ \dfrac{\alpha\varepsilon_2}{2\varepsilon_1}, & \text{if } \sqrt{\alpha}\varepsilon_2 > \sqrt{\rho\varepsilon_1}, \end{cases} \quad \text{and} \quad \theta_2 = \begin{cases} \dfrac{\sqrt{\rho\alpha}}{\sqrt{\varepsilon}_1}, & \text{if } \sqrt{\alpha}\varepsilon_2 \le \sqrt{\rho\varepsilon_1}, \\ \dfrac{\rho}{2\varepsilon_2}, & \text{if } \sqrt{\alpha}\varepsilon_2 > \sqrt{\rho\varepsilon_1}. \end{cases} \tag{2.9}$$

Consider the Case (ii): $\sqrt{\alpha}\varepsilon_2 > \sqrt{\rho\varepsilon_1}$.

Let $v^*(x) = v_0^*(x) + \varepsilon_1 v_1^*(x) + \varepsilon_1^2 v_2^*(x)$, where $v_0^*(x)$, $v_1^*(x)$ and $v_2^*(x)$ are the solutions of the following problems, respectively:

$$\varepsilon_2 a(x) v_0^{*'}(x) - b(x)v_0^*(x) = f(x), \quad x \in (\Omega^- \cup \Omega^+), \quad v_0^*(0) = y(0), v_0^*(1) = y(1),$$

$$\varepsilon_2 a(x) v_1^{*'}(x) - b(x)v_1^*(x) = -v_0^{*''}(x), \quad x \in (\Omega^- \cup \Omega^+), \quad v_1^*(0) = 0 = v_1^*(1) = 0,$$

$$\mathcal{L}v_2^*(x) = -v_1^{*''}(x), \quad x \in (\Omega^- \cup \Omega^+),$$

$$v_2^*(0) = v_2^*(1) = 0, \ v_2^*(d-), \ v_2^*(d+) \text{ are chosen,}$$

where $v_2^*(x) \in \mathcal{C}^0(\overline{\Omega}) \cap \mathcal{C}^1(\Omega) \cap \mathcal{C}^2(\Omega^- \cup \Omega^+)$.

Lemmas 2.8 and 2.9 can be proved using the principles and methods adopted in [2,15].

Lemma 2.8. *The regular component $v^*(x)$ satisfies the following bounds*

$$\|v^{*(k)}(x)\|_{\Omega\setminus\{d\}} \leq C\left(1+\left(\frac{\varepsilon_1}{\varepsilon_2}\right)^{2-k}\right), \quad k=0,1,2 \text{ and } 3. \tag{2.10}$$

Lemma 2.9. *The singular components $w_l^*(x)$ and $w_r^*(x)$ satisfy the following bounds*

$$\|w_l^{*(k)}(x)\|_{\Omega\setminus\{d\}} \leq C\begin{cases}\left(\frac{1}{\varepsilon_2}\right)^k Ce^{-\theta_2 x}, & x\in\Omega^-,\\ \left(\frac{\varepsilon_2}{\varepsilon_1}\right)^k Ce^{-\theta_1(x-d)}, & x\in\Omega^+,\end{cases} \quad k=0,1,2 \text{ and } 3,$$

$$\|w_r^{*(k)}(x)\|_{\Omega\setminus\{d\}} \leq C\begin{cases}\left(\frac{\varepsilon_2}{\varepsilon_1}\right)^k Ce^{-\theta_1(d-x)}, & x\in\Omega^-,\\ \left(\frac{1}{\varepsilon_2}\right)^k Ce^{-\theta_2(1-x)}, & x\in\Omega^+,\end{cases} \quad k=0,1,2 \text{ and } 3,$$

with θ_1 and θ_2 as in (2.9).

The unique solution $y(x)$ of the problem (1.1)–(1.4) is now given by

$$y(x)=\begin{cases} v^{*-}(x)+w_l^{*-}(x)+w_r^{*-}(x), & x\in\Omega^-,\\ v^{*-}(d-)+w_l^{*-}(d-)+w_r^{*-}(d-)=v^{*+}(d+)+w_l^{*+}(d+)+w_r^{*+}(d+), & x=d,\\ v^{*+}(x)+w_l^{*+}(x)+w_r^{*+}(x), & x\in\Omega^+.\end{cases}$$

Remark. The following properties of θ_1 and θ_2 are significant. The values of θ_1 and θ_2 used in the previous lemmas are required in order to estimate the error in the numerical approximations. Let θ_1,θ_2 be defined as in (2.9), then they are respectively the positive roots of the equations $\varepsilon_1\theta_1^2-\varepsilon_2\alpha_1\theta_1-\gamma=0$ and $\varepsilon_1\theta_2^2+\varepsilon_2\alpha_2\theta_2-\gamma=0$.

3. Discrete problem

The continuous problem is discretized using finite difference methods with a suitable Shishkin mesh. On $\overline{\Omega}$ a piecewise uniform mesh size N (let N be even and $N\geq 8$) is determined as follows. The domain $\overline{\Omega}$ is subdivided into six subintervals as $\overline{\Omega}=[0,\sigma_1]\cup[\sigma_1,d-\sigma_2]\cup[d-\sigma_2,d]\cup[d,d+\sigma_3]\cup[d+\sigma_3,1-\sigma_4]\cup[1-\sigma_4,1]$. The subintervals $[0,\sigma_1]$, $[d-\sigma_2,d]$, $[d,d+\sigma_3]$ and $[1-\sigma_4,1]$ are scaled with a uniform mesh of $N/8$ mesh intervals, while $[\sigma_1,d-\sigma_2]$ and $[d+\sigma_3,1-\sigma_4]$ have a uniform mesh with $N/4$ mesh intervals. The step sizes in each subinterval are defined by $\overline{h}_1=8\sigma_1/N$, $\overline{h}_2=4(d-\sigma_1-\sigma_2)/N$, $\overline{h}_3=8\sigma_2/N$, $\overline{h}_4=8\sigma_3/N$, $\overline{h}_5=4(1-d-\sigma_3-\sigma_4)/N$ and $\overline{h}_6=8\sigma_4/N$. Let $h_i=x_i-x_{i-1}$, $i=1,2,\ldots,N$ are the mesh steps.

The interior points of the mesh are denoted by

$$\Omega^N=\{x_i: 1\leq i\leq N/2-1\}\cup\{x_i: N/2+1\leq i\leq N-1\}.$$

If the discontinuity is assumed at the point $x_{N/2}$ then the mesh points are denoted by $\overline{\Omega}^N=\{x_i\}_0^N$. The transition values in $\overline{\Omega}$ are chosen as

$$\begin{cases}\sigma_1=\min\left\{\frac{d}{4},\frac{2}{\theta_2}\ln N\right\}, \quad \sigma_2=\min\left\{\frac{d}{4},\frac{2}{\theta_1}\ln N\right\},\\ \sigma_3=\min\left\{\frac{1-d}{4},\frac{2}{\theta_1}\ln N\right\}, \quad \sigma_4=\min\left\{\frac{1-d}{4},\frac{2}{\theta_2}\ln N\right\},\end{cases} \tag{3.1}$$

where θ_1,θ_2, had been defined in (2.9).

On the piecewise uniform mesh $\overline{\Omega}^N$ the BVP (1.1)–(1.4) is discretized using standard upwind finite difference scheme as follows:

Consider a mesh function $Y(x_i)$, $\forall\, x_i\in\Omega^N$ such that

$$\mathcal{L}^N Y(x_i)\equiv\varepsilon_1\delta^2Y(x_i)+\varepsilon_2 a(x_i)D^*Y(x_i)-b(x_i)Y(x_i)=f(x_i), \tag{3.2}$$

$$Y(0)=y(0), \quad Y(1)=y(1), \tag{3.3}$$

$$D^-Y(x_{N/2})=D^+Y(x_{N/2}), \tag{3.4}$$

where

$$D^+Y(x_i) = \frac{Y(x_{i+1}) - Y(x_i)}{x_{i+1} - x_i}, \qquad D^-Y(x_i) = \frac{Y(x_i) - Y(x_{i-1})}{x_i - x_{i-1}},$$

$$D^*Y(x_i) = \begin{cases} D^-Y(x_i), & i < N/2, \\ D^+Y(x_i), & i > N/2, \end{cases} \qquad \delta^2 Y(x_i) = \frac{2(D^+Y(x_i) - D^-Y(x_i))}{x_{i+1} - x_{i-1}}.$$

The next lemma reveals that the finite difference operator $\mathcal{L}^N$ has properties equivalent to those of the continuous differential operator $\mathcal{L}$ defined in Section 2.

Lemma 3.1. *Suppose that a mesh function $Y(x_i)$ satisfies*

$$Y(0) \geq 0, \qquad Y(1) \geq 0, \qquad \mathcal{L}^N Y(x_i) \leq 0, \quad \forall\, x_i \in \Omega^N,$$
$$D^+Y(x_{N/2}) - D^-Y(x_{N/2}) \leq 0\,.$$

Then we have that $Y(x_i) \geq 0,\ \forall\, x_i\ \in \overline{\Omega}^N$.

Proof. Let x_k be any point at which $Y(x_k)$ attains its minimum value on $\overline{\Omega}^N$. If $Y(x_k) > 0$ then the proof is trivial. Suppose that $Y(x_k) < 0$, then the proof is concluded by the method of contradiction. Here $x_k \in \Omega^N$ or $x_k = x_{N/2}$. If $x_k \in \Omega^N$ it is clear that $x_k \neq x_{N/2}$ and

$$D^-Y(x_k) \leq 0 \leq D^+Y(x_k).$$

Now

$$\mathcal{L}^N Y(x_k) = \begin{cases} \varepsilon_1 \delta^2 Y(x_k) + \varepsilon_2 a(x_k) D^-Y(x_k) - b(x_k) Y(x_k) > 0, & \text{if } x_k < x_{N/2}, \\ \varepsilon_1 \delta^2 Y(x_k) + \varepsilon_2 a(x_k) D^+Y(x_k) - b(x_k) Y(x_k) > 0, & \text{if } x_k > x_{N/2}, \end{cases}$$

which is a contradiction. Due to the boundary values considered, the only other possibility to consider is $x_k = x_{N/2}$ which gives

$$D^-Y(x_{N/2}) \leq 0 \leq D^+Y(x_{N/2}) \leq D^-Y(x_{N/2}).$$

This shows that

$$Y(x_{N/2-1}) = Y(x_{N/2}) = Y(x_{N/2+1}) < 0,$$

and then

$$\mathcal{L}^N Y(x_{N/2-1}) > 0.$$

This contradicts our result. Hence $Y(x_i) \geq 0$ for all $x_i \in \Omega^N$. □

Lemma 3.2. *If $Y(x_i)$ is any mesh function with $x_i \in \overline{\Omega}^N$, verifying (3.2)–(3.4), then $\|Y\|_{\overline{\Omega}^N} \leq C$.*

Proof. Define the mesh function

$$\phi^{\pm}(x_i) = \psi(x_i) \pm Y(x_i),$$

where

$$\psi(x_i) = \begin{cases} \max\{|Y(0)|, |Y(1)|\} + \dfrac{x_i \|f\|}{(\xi x_{N/2})} \pm Y(x_i), & \text{for } 1 \leq i \leq N/2 - 1, \\ \max\{|Y(0)|, |Y(1)|\} + \dfrac{(1 - x_i)\|f\|}{\xi(1 - x_{N/2})} \pm Y(x_i), & \text{for } N/2 + 1 \leq i \leq N - 1, \end{cases}$$

with $\xi = \min\left\{\dfrac{\alpha_1}{x_{N/2}}, \dfrac{\alpha_2}{1 - x_{N/2}}\right\}$.

We have that $\phi^{\pm}(0)$, $\phi^{\pm}(1)$ are non-negative, and for each $x_i \in \Omega^N$ it is

$$\mathcal{L}^N \phi^{\pm}(x_i) = -b(x_i)\psi(x_i) \pm \mathcal{L}^N Y(x_i) \leq 0, \quad \text{if } x_i < x_{N/2},$$
$$\mathcal{L}^N \phi^{\pm}(x_i) = -b(x_i)\psi(x_i) \pm \mathcal{L}^N Y(x_i) \leq 0, \quad \text{if } x_i > x_{N/2}.$$

Furthermore, since $Y(x_i) \in \mathcal{C}^1(\Omega)$,

$$\left[\phi^{\pm}\right](x_{N/2}) = \pm [Y](x_{N/2}) = 0 \qquad \text{and} \qquad \left[\phi^{\pm\prime}\right](x_{N/2}) = \frac{\|f\|}{\varepsilon_1(1 - x_{N/2})} + \frac{\|f\|}{\varepsilon_1(x_{N/2})} \leq 0.$$

Applying the discrete minimum principle, it follows that $\phi^{\pm}(x_i) \geq 0$ for all $x_i \in \overline{\Omega}^N$. This leads to the required result

$$\|Y\|_{\overline{\Omega}^N} \leq C. \quad \square$$

4. Decomposition and bounds for the discrete solution

The error $|e(x_i)| = |Y(x_i) - y(x_i)|$ at each mesh point $x_i \in \overline{\Omega}^N$ is constructed. In order to bound the nodal error $|e(x_i)|$, we decompose the solution of the discrete problem (3.2)–(3.4) as $Y(x_i) = V^*(x_i) + W_l^*(x_i) + W_r^*(x_i)$ in a way similar to the decomposition of continuous solutions. To obtain sharper bounds the discrete regular component $V^*(x_i)$ and singular components $W_l^*(x_i)$, $W_r^*(x_i)$ are further decomposed as $V^{*-}(x_i)$ and $V^{*+}(x_i)$, which approximate $V^*(x_i)$ respectively to the left and right sides of the point of discontinuity $x_{N/2} = d$ while the mesh functions $W_l^{*-}(x_i)$, $W_l^{*+}(x_i)$ and $W_r^{*-}(x_i)$, $W_r^{*+}(x_i)$ approximate $W_l^*(x_i)$ and $W_r^*(x_i)$ respectively on either side of the point of discontinuity $d = x_{N/2}$. These mesh functions help in deriving the convergence of the nodal error $|e(x_i)|$ in the boundary and interior layers.

The regular discrete component $V^*(x_i)$ is defined as

$$V^*(x_i) = \begin{cases} V^{*-}(x_i), & \text{for } 1 \leq i \leq N/2 - 1, \\ V^{*+}(x_i), & \text{for } N/2 + 1 \leq i \leq N - 1, \end{cases}$$

where, $V^{*-}(x_i)$ and $V^{*+}(x_i)$ are respectively, the solutions of the following discrete problems:

$$\mathcal{L}^N V^{*-}(x_i) = f(x_i), \quad \text{for } 1 \leq i \leq N/2 - 1, \quad V^{*-}(0) = v^*(0), \quad V^{*-}(x_{N/2}) = v^*(d-),$$

and

$$\mathcal{L}^N V^{*+}(x_i) = f(x_i), \quad \text{for } N/2 + 1 \leq i \leq N - 1, \quad V^{*+}(x_{N/2}) = v^*(d+), \quad V^{*+}(1) = v^*(1).$$

Further the discrete singular components $W_l^{*-}(x_i)$, $W_l^{*+}(x_i)$, $W_r^{*-}(x_i)$ and $W_r^{*+}(x_i)$ are defined as

$$W^*(x_i) = W_l^*(x_i) + W_r^*(x_i) = \begin{cases} (W_l^{*-} + W_r^{*-})(x_i), & \text{for } 1 \leq i \leq N/2 - 1, \\ (W_l^{*+} + W_r^{*+})(x_i), & \text{for } N/2 + 1 \leq i \leq N - 1, \end{cases}$$

where, $W_l^{*-}(x_i)$, $W_l^{*+}(x_i)$, $W_r^{*-}(x_i)$ and $W_r^{*+}(x_i)$ are the solutions of the following discrete problems:

$$\begin{aligned}
&\mathcal{L}^N W_l^{*-}(x_i) = 0, \quad \text{for } 1 \leq i \leq N/2 - 1, \quad W_l^{*-}(0) = w_l^{*-}(0), \quad W_l^{*-}(x_{N/2}) = w_l^{*-}(x_{N/2}), \\
&\mathcal{L}^N W_l^{*+}(x_i) = 0, \quad \text{for } N/2 + 1 \leq i \leq N - 1, \quad W_l^{*+}(x_{N/2}) = w_l^{*+}(x_{N/2}), \quad W_l^{*+}(1) = w_l^{*+}(1), \\
&\mathcal{L}^N W_r^{*-}(x_i) = 0, \quad \text{for } 1 \leq i \leq N/2 - 1, \quad W_r^{*-}(0) = 0, \quad W_r^{*-}(x_{N/2}) = w_r^{*-}(x_{N/2}), \\
&\mathcal{L}^N W_r^{*+}(x_i) = 0, \quad \text{for } N/2 + 1 \leq i \leq N - 1, \quad W_r^{*+}(x_{N/2}) = 0, \quad W_r^{*+}(1) = w_r^{*+}(1).
\end{aligned}$$

The solution $Y(x_i)$ of the discrete problem (3.2)–(3.4) could now be defined as

$$Y(x_i) = \begin{cases} \left(V^{*-} + W_l^{*-} + W_r^{*-}\right)(x_i), & \text{for } 1 \leq i \leq N/2 - 1, \\ \left(V^{*-} + W_l^{*-} + W_r^{*-}\right)(x_i) = \left(V^{*+} + W_l^{*+} + W_r^{*+}\right)(x_i), & \text{for } i = N/2, \\ \left(V^{*+} + W_l^{*+} + W_r^{*+}\right)(x_i), & \text{for } N/2 + 1 \leq i \leq N - 1. \end{cases}$$

Lemma 4.1. *There are some bounds on $W_l^{*-}(x_i)$, $W_l^{*+}(x_i)$, $W_r^{*-}(x_i)$ and $W_r^{*+}(x_i)$ given by*

$$\begin{aligned}
&| W_l^{*-}(x_i) | \leq \psi_{li}^- = C \prod_{k=1}^{i} (1 + \theta_2 h_k)^{-1}, \quad \psi_{l0}^- = C_1, \\
&| W_l^{*+}(x_i) | \leq \psi_{li}^+ = C \prod_{k=N/2+1}^{i} (1 + \theta_1 h_k)^{-1}, \quad \psi_{lN/2}^+ = C_1, \\
&| W_r^{*-}(x_i) | \leq \psi_{ri}^- = C \prod_{k=i+1}^{N/2} (1 + \theta_1 h_k)^{-1}, \quad \psi_{rN/2}^- = C_1, \\
&| W_r^{*+}(x_i) | \leq \psi_{ri}^+ = C \prod_{k=i+1}^{N} (1 + \theta_2 h_k)^{-1}, \quad \psi_{rN}^+ = C_1,
\end{aligned}$$

where $h_i = x_i - x_{i-1}$.

Proof. Define the barrier functions

$$\xi_{li}^{-} = \psi_{li}^{-} \pm W_l^{*-}(x_i) \qquad \text{and} \qquad \xi_{ri}^{-} = \psi_{ri}^{-} \pm W_r^{*-}(x_i),$$

where

$$\psi_{li}^{-} = \begin{cases} \prod_{j=1}^{i} \left(1+\theta_2 h_j\right)^{-1}, & 1 \le i \le N/2, \\ 1, & i = 0, \end{cases}$$

$$\psi_{ri}^{-} = \begin{cases} \prod_{j=i+1}^{d} \left(1+\theta_1 h_j\right)^{-1}, & 0 \le i < N/2, \\ 1, & i = N/2, \end{cases}$$

with θ_1, θ_2 as were defined in (2.9) of Section 2.

Now $\xi_{l0} > 0$ and $\xi_{ld} > 0$. To prove that $\mathcal{L}^N \xi_{li}^{-} \le 0$ we apply the discrete operator (3.2) on ξ_{li}^{-}. With $\mathcal{L}^N W_l^{*-} = 0$ and $\mathcal{L}^N W_r^{*-} = 0$, we have

$$\mathcal{L}^N \xi_{li}^{-} = \psi_{li+1}^{-} \left[\varepsilon_1 \theta_2^2 \left(\frac{h_{i+1}}{\hat{h}_i} - 2 \right) + \left(2\varepsilon_1 \theta_2^2 + \varepsilon_2 a_i \theta_2 - \gamma \right) - \gamma \theta_2 h_{i+1} \right] \le 0,$$

where $\hat{h}_i = \dfrac{h_i + h_{i+1}}{2}$.

Hence

$$\mathcal{L}^N \xi_{li}^{-} \le \psi_{li+1}^{-} \left(2\varepsilon_1 \theta_2^2 + \varepsilon_2 a_i \theta_2 - \gamma \right) \le 0.$$

Considering the θ values from (2.9), for $\sqrt{\alpha}\varepsilon_2 \le \sqrt{\rho \varepsilon_1}$ we obtain

$$\begin{aligned} \mathcal{L}^N \xi_{li}^{-} &\le \psi_{li+1}^{-} \left(\frac{\rho\alpha}{2} + \frac{\rho a_i}{2} - b_i \right) \\ &\le \psi_{li+1}^{-} \left(\rho a_i - b_i \right) \le \psi_{li+1}^{-} a_i \left(\rho - \frac{\gamma}{a_i} - 2\gamma \right) \le 0. \end{aligned}$$

When $\sqrt{\alpha}\varepsilon_2 > \sqrt{\rho \varepsilon_1}$ we get

$$\mathcal{L}^N \xi_{li}^{-} \le \psi_{li+1}^{-} \left(a_i + \frac{\rho a_i}{2} - \gamma \right) \le \psi_{li+1}^{-} \left(a_i \frac{b_i}{2} \right) \le 0.$$

The discrete minimum principle defined in [15] for the continuous case proves that $\xi_l^{-}(x_i) \ge 0$, and hence $W_l^{*-}(x_i) \le C \prod_{k=1}^{i} (1+\theta_2 h_k)^{-1}$.

Applying the upwind difference scheme to the right layer barrier function ξ_{ri}^{-}, we get

$$\begin{aligned} \mathcal{L}^N \xi_{ri}^{-} &= \frac{\psi_{ri}^{-}}{1+\theta_1 h_i} \left[2\varepsilon_1 \theta_1^2 \left(\frac{h_i}{\hat{h}_i} - 1 \right) + \left(2\varepsilon_1 \theta_1^2 - \varepsilon_2 a_i \theta_1 - \gamma \right) (1+\theta_1 h_i) - \gamma (1+\theta_1 h_i) \right] \\ &\le \frac{\psi_{ri}^{-}}{1+\theta_1 h_i} \left(2\varepsilon_1 \theta_1^2 - \varepsilon_2 a_i \theta_1 - \gamma \right) \le 0. \end{aligned}$$

Considering the value of θ_1 in (2.9), for $\sqrt{\alpha}\varepsilon_2 \le \sqrt{\rho \varepsilon_1}$ we obtain

$$\mathcal{L}^N \xi_{ri}^{-} \le \frac{\psi_{ri}^{-}}{1+\theta_1 h_i} \left(\frac{\rho\alpha}{2} - \gamma \right) \le 0.$$

When $\sqrt{\alpha}\varepsilon_2 > \sqrt{\rho \varepsilon_1}$ we get

$$\mathcal{L}^N \xi_{ri}^{-} \le \frac{\psi_{ri}^{-}}{1+\theta_1 h_i} \left(\frac{\alpha^2 \varepsilon_2^2}{2\varepsilon_1} [\alpha - a_i] - \gamma \right) \le 0.$$

Now $\xi_{r0}^{-} > 0$ and $\xi_{rd}^{-} > 0$ and $\mathcal{L}^N \xi_{ri}^{-} \le 0$. Applying the discrete minimum principle defined in [15], we prove that $\xi_{ri}^{-}(x_i) \ge 0$ and hence $W_r^{-}(x_i) \le C \prod_{k=i+1}^{N/2} (1+\theta_1 h_k)^{-1}$. Similarly, by defining the corresponding barrier functions ξ_{li}^{+} and ξ_{ri}^{+} we could prove the results for $W_l^{+}(x_i)$ and $W_r^{+}(x_i)$ for $N/2+1 \le i \le N-1$. □

5. Truncation error analysis

Lemma 5.1. *The error of the regular component satisfies the following estimate for each mesh point $x_i \in \Omega^N$*

$$\|V^* - v^*\| \leq CN^{-1}, \tag{5.1}$$

where V^* and v^* are the solutions of the discrete and continuous decompositions defined in Sections 2 and 4 respectively.

Proof. Applying the regular arguments on the truncation error and the bounds on $v^*(x)$ for both the cases $\sqrt{\alpha}\varepsilon_2 \leq \sqrt{\rho\varepsilon_1}$ and $\sqrt{\alpha}\varepsilon_2 > \sqrt{\rho\varepsilon_1}$ we get

$$\begin{aligned}
|\mathcal{L}^N(V^{*-} - v^{*-})(x_i)| &= |\mathcal{L}^N v^{*-}(x_i) - f(x_i)| \\
&\leq \left|\varepsilon_1\left(\delta^2 - \frac{d^2}{dx^2}\right)\right| + \left|\varepsilon_2 a(x_i)\left(D^+ - \frac{d}{dx}\right)\right| \\
&\leq C\varepsilon_1 (x_{i+1} - x_i)^2 |v^{-(3)}| + \varepsilon_2 a(x_i)(x_{i+1} - x_i)|v^{-(2)}| \\
&\leq CN^{-1}.
\end{aligned}$$

Similarly, we could prove that

$$|\mathcal{L}^N(V^{*+} - v^{*+})(x_i)| \leq CN^{-1}, \quad \text{for } N/2 + 1 \leq i \leq N - 1.$$

Define the barrier function

$$\psi_i^{\pm} = CN^{-1} \pm (V^{*-} - v^{*-})(x_i), \quad \forall\, x_i \in \overline{\Omega}^N.$$

It is clear that $\psi^{\pm}(0) \geq 0$ and $\psi^{\pm}(1) \geq 0$. For greater values of C, $\mathcal{L}^N\psi_i^{\pm} \leq 0$. Applying Lemma 3.1 on $\psi_i^{\pm}$ we get $\psi_i^{\pm} \geq 0$ for $0 \leq i \leq N$. Combining the above results, we obtain

$$\|(V^* - v^*)\| \leq CN^{-1}, \quad \forall\, x_i \in \Omega^N. \quad \square$$

Remark. The above lemma holds relevant irrespective of the nature of the relation between ε_1 and ε_2. This is followed by the derivation of estimates for the singular component. It has to be noted that there is a unique formation of boundary layers in the considered problem due to the discontinuity assumed in the convection coefficient. If $a(x)$ behaves as in (1.3) there is a shift in the occurrence of boundary layer from ε_2 to $(\varepsilon_1/\varepsilon_2)$ on the left side of the point of discontinuity and $(\varepsilon_1/\varepsilon_2)$ on the right side of the point of discontinuity, unlike the case when $a(x)$ is continuous and $f(x)$ has a jump discontinuity [16]. These shifts in the interior layers and the boundary layers make the computation difficult and the error analysis section has to be dealt very carefully to prove the required results.

Lemma 5.2. *At each mesh point $x_i \in \Omega^N$ the right singular component of the truncation error satisfies the following estimate*

$$\|W_r^* - w_r^*\| \leq \begin{cases} CN^{-1}(\ln N), & \text{if } \sqrt{\alpha}\varepsilon_2 \leq \sqrt{\rho\varepsilon_1}, \\ CN^{-1}(\ln N)^2, & \text{if } \sqrt{\alpha}\varepsilon_2 > \sqrt{\rho\varepsilon_1}. \end{cases}$$

Proof. Using the classical argument for the truncation error and Lemma 2.4, we obtain

$$\begin{aligned}
|\mathcal{L}^N(W_r^{*-} - w_r^{*-})(x_i)| &= |(\mathcal{L}^N - \mathcal{L})w_r^{*-}(x_i)| \\
&\leq C(h_{i+1} + h_i)\varepsilon_1\|(w_r^{*-})^3\| + \varepsilon_2\|(w_r^{*-})^2\| \\
&\leq C(h_{i+1} + h_i)\left\{\frac{1}{\sqrt{\varepsilon_1}}\left(1 + \left(\frac{\varepsilon_2}{\sqrt{\varepsilon_1}}\right)^3\right) + \frac{\varepsilon_2}{\varepsilon_1}\left(1 + \left(\frac{\varepsilon_2}{\sqrt{\varepsilon_1}}\right)^2\right)\right\} \\
&\leq C(h_{i+1} + h_i)\frac{1}{\sqrt{\varepsilon_1}}\left(1 + \left(\frac{\varepsilon_2}{\sqrt{\varepsilon_1}}\right)^3\right).
\end{aligned} \tag{5.2}$$

If $\sigma_2 = d/4$, the mesh is uniform and $\theta_1 \leq 16(\ln N)$. Hence (5.2) reduces to

$$|\mathcal{L}^N(W_r^{*-} - w_r^{*-})(x_i)| \leq \begin{cases} CN^{-1}\left(\dfrac{1}{\sqrt{\varepsilon_1}}\right), & \text{if } \sqrt{\alpha}\varepsilon_2 \leq \sqrt{\rho\varepsilon_1}, \\ CN^{-1}\left(\dfrac{\varepsilon_2^3}{\varepsilon_1^2}\right), & \text{if } \sqrt{\alpha}\varepsilon_2 > \sqrt{\rho\varepsilon_1}. \end{cases} \tag{5.3}$$

The error in the fine mesh region $(d - \sigma_2, d)$ and the coarse mesh region $(0, d - \sigma_2]$ are analyzed using the bounds defined in Lemmas 2.7 and 2.9. On simplifying (5.2) we obtain

$$|\mathcal{L}^N(W_r^{*-} - w_r^{*-})(x_i)| \leq C_1 N^{-1}\ln N + C_2 N^{-1}\left(\frac{\varepsilon_2}{\varepsilon_1}\right)\ln N. \tag{5.4}$$

Using the values of θ_1 and $\sigma_2 \leq \dfrac{2}{\theta_1}\ln N$, we get

$$|\mathcal{L}^N(W_r^{*-} - w_r^{*-})(x_i)| \leq \begin{cases} CN^{-1}\ln N, & \text{if } \sqrt{\alpha}\varepsilon_2 \leq \sqrt{\rho\varepsilon_1}, \\ CN^{-1}\varepsilon_2(\ln N)^2, & \text{if } \sqrt{\alpha}\varepsilon_2 > \sqrt{\rho\varepsilon_1}. \end{cases}$$

Using the barrier function technique and discrete minimum principle we derive

$$\|(W_r^{*-} - w_r^{*-})\| \leq \begin{cases} CN^{-1}\ln N, & \text{if } \sqrt{\alpha}\varepsilon_2 \leq \sqrt{\rho\varepsilon_1}, \\ CN^{-1}(\ln N)^2, & \text{if } \sqrt{\alpha}\varepsilon_2 > \sqrt{\rho\varepsilon_1}. \end{cases} \tag{5.5}$$

Following similar arguments in the domain $(d, 1-\sigma_4]$ and $(1-\sigma_4, 1)$ we obtain

$$\|(W_r^{*+} - w_r^{*+})\| \leq \begin{cases} CN^{-1}\ln N, & \text{if } \sqrt{\alpha}\varepsilon_2 \leq \sqrt{\rho\varepsilon_1}, \\ CN^{-1}(\ln N)^2, & \text{if } \sqrt{\alpha}\varepsilon_2 > \sqrt{\rho\varepsilon_1}, \end{cases} \tag{5.6}$$

Combining the results (5.5) and (5.6) the desired result is obtained. □

Lemma 5.3. *At each mesh point $x_i \in \Omega^N$ the left singular component of the truncation error satisfies the following estimate*

$$\|(W_l^{*-} - w_l^{*-})\| \leq \begin{cases} CN^{-1}\ln N, & \text{if } \sqrt{\alpha}\varepsilon_2 \leq \sqrt{\rho\varepsilon_1}, \\ CN^{-1}(\ln N)^2, & \text{if } \sqrt{\alpha}\varepsilon_2 > \sqrt{\rho\varepsilon_1}. \end{cases}$$

Proof. Using the derivative estimate, we have

$$|\mathcal{L}^N(W_l^{*-} - w_l^{*-})(x_i)| \leq C(h_{i+1} + h_i)\left\{\frac{1}{\sqrt{\varepsilon_1}}\left(1 + \left(\frac{\varepsilon_2}{\sqrt{\varepsilon_1}}\right)^3\right)\right\}. \tag{5.7}$$

We begin with the case $\sqrt{\alpha}\varepsilon_2 \leq \sqrt{\rho\varepsilon_1}$. If $\sigma_1 = \dfrac{d}{4}$, with $\sqrt{\alpha}\varepsilon_2/\sqrt{\varepsilon_1} \leq \theta_2 \leq 16\ln N$ we obtain the following bounds on the left singular component given by

$$|\mathcal{L}^N(W_l^{*-} - w_l^{*-})(x_i)| \leq \frac{C}{\sqrt{\varepsilon_1}}(h_{i+1} + h_i) \leq CN^{-1}\ln N.$$

When $\sigma_1 < \dfrac{d}{4}$, we have to analyze the error in the fine and coarse mesh regions separately. Following the methods applied in [15] we could prove the bound for the coarse mesh region $[\sigma_1, d)$ given by

$$|\mathcal{L}^N(W_l^{*-} - w_l^{*-})(x_i)| \leq CN^{-1}\frac{\sqrt{\rho\alpha}}{\sqrt{\varepsilon_1}} \leq CN^{-1}\ln N.$$

In the fine mesh region $(0, \sigma_1)$ the inequality (5.7) still holds and we have $h_i = h_{i+1} = \dfrac{16(N^{-1}\ln N)}{\theta_2}$. Using the value of θ_2 we have $\dfrac{\sqrt{\rho\alpha}(h_{i+1} - h_i)}{\sqrt{\varepsilon_1}} \leq CN^{-1}\ln N$. Hence

$$|\mathcal{L}^N(W_l^{*-} - w_l^{*-})(x_i)| \leq CN^{-1}\frac{\sqrt{\rho\alpha}}{\sqrt{\varepsilon_1}} \leq CN^{-1}\ln N.$$

Consider the case $\sqrt{\alpha}\varepsilon_2 > \sqrt{\rho\varepsilon_1}$.
Following the methods constructed for the error bounds in [15] when the transition point $\sigma_2 = d/4$, and $\dfrac{\rho}{\varepsilon_2} \leq \theta_2 \leq 16(\ln N)$ we obtain

$$|\mathcal{L}^N(W_l^{*-} - w_l^{*-})(x_i)| \leq CN^{-1}\left(\frac{\rho}{{\varepsilon_2}^2}\right) \leq CN^{-1}(\ln N)^2.$$

For the coarse mesh region $[\sigma_1, d)$, if the transition point $\sigma_1 < \dfrac{d}{4}$ the error bound in (5.7) still holds. In the fine mesh region $(0, \sigma_1)$ the inequality (5.7) reduces to

$$|\mathcal{L}^N(W_l^{*-} - w_l^{*-})(x_i)| \leq C\frac{{h_{i+1} + h_i}^2}{\varepsilon_2}.$$

Since $h_{i+1} = h_i = \left(\dfrac{16}{\theta_2}\right)\ln N$ and using the value of θ_2 the following error bound is obtained for the left singular component

$$|\mathcal{L}^N(W_l^{*-} - w_l^{*-})(x_i)| \leq CN^{-1}(\ln N)^2.$$

Using the mesh function technique and discrete minimum principle we can prove that

$$\|(W_l^{*-} - w_l^{*-})\| \leq \begin{cases} CN^{-1}\ln N, & \text{if } \sqrt{\alpha}\varepsilon_2 \leq \sqrt{\rho\varepsilon_1}, \\ CN^{-1}(\ln N)^2, & \text{if } \sqrt{\alpha}\varepsilon_2 > \sqrt{\rho\varepsilon_1}. \end{cases}$$

Similarly, we can prove the result for $N/2+1 \leq i < N$ by taking appropriate transition parameter σ_3 to obtain

$$\|\mathcal{L}^N(W_l^{*+} - w_l^{*+})\| \leq \begin{cases} CN^{-1}\ln N, & \text{if } \sqrt{\alpha}\varepsilon_2 \leq \sqrt{\rho\varepsilon_1}, \\ CN^{-1}(\ln N)^2, & \text{if } \sqrt{\alpha}\varepsilon_2 > \sqrt{\rho\varepsilon_1}. \end{cases}$$

In particular $d = 1/2$ could be seen as a special case here since, $\sigma_1 = \sigma_2 = \sigma_3 = \sigma_4 = 1/8$. If $\sigma_1 < d/4$ and , $\sigma_2 < d/4$, then the mesh is piecewise uniform.

Combining all the results analyzed above we can say that

$$\|W^* - w^*\| \leq \begin{cases} CN^{-1}\ln N, & \text{if } \sqrt{\alpha}\varepsilon_2 \leq \sqrt{\rho\varepsilon_1}, \\ CN^{-1}(\ln N)^2, & \text{if } \sqrt{\alpha}\varepsilon_2 > \sqrt{\rho\varepsilon_1}. \end{cases} \quad \square$$

Lemma 5.4. *The error $e(x_{N/2})$ estimated at the point of discontinuity $x_{N/2} = d$ satisfies the following estimate*

$$|(D^+ - D^-)(Y(x_{N/2}) - y(x_{N/2}))| \leq \begin{cases} \dfrac{\rho\alpha\sigma}{N\varepsilon_1}, & \text{if } \sqrt{\alpha}\varepsilon_2 \leq \sqrt{\rho\varepsilon_1}, \\ \dfrac{\alpha\sigma\varepsilon_2^2}{N\varepsilon_1^2}, & \text{if } \sqrt{\alpha}\varepsilon_2 > \sqrt{\rho\varepsilon_1}, \end{cases}$$

where $\sigma = min\{\sigma_2, \sigma_3\}$.

Proof. Consider

$$\begin{aligned} |(D^+ - D^-)(Y(x_{N/2}) - y(x_{N/2}))| &= |(D^- - D^+)(y(x_i) + [y'](x_i))| \\ &\leq |y'(x_{N/2}) - D^+y(x_{N/2})| + |y'(x_{N/2}) - D^-y(x_{N/2})|. \end{aligned}$$

We know that, $(D^+ - D^-)Y(x_{N/2}) = 0$. Let $\bar{h}_3 = 8\sigma_2/N$ and $\bar{h}_4 = 8\sigma_3/N$ be the mesh sizes on either side of $x_{N/2}$. Then, we obtain

$$\begin{aligned} |(D^+ - D^-)(Y(x_{N/2}) - y(x_{N/2}))| &= |(D^- - D^+)y(x_{N/2})| \\ &\leq \left|\left(\frac{d}{dx} - D^-\right)y(x_{N/2})\right| + \left|\left(\frac{d}{dx} - D^+\right)y(x_{N/2})\right| \\ &\leq \begin{cases} \dfrac{C\bar{h}}{\varepsilon_1}, & \text{if } \sqrt{\alpha}\varepsilon_2 \leq \sqrt{\rho\varepsilon_1}, \\ \dfrac{C\bar{h}\varepsilon_2^2}{\varepsilon_1^2}, & \text{if } \sqrt{\alpha}\varepsilon_2 > \sqrt{\rho\varepsilon_1}, \end{cases} \end{aligned}$$

where $\bar{h} = \min\{h_3, h_4\}$. $\square$

Remark. When the sign of the discontinuous convection coefficient $a(x)$ is reversed, the result at the point of discontinuity $x_{N/2}$ takes the form

$$|(D^+ - D^-)e(x_{N/2})| \leq \begin{cases} \dfrac{\rho\alpha\sigma}{N\varepsilon_1}, & \text{if } \sqrt{\alpha}\varepsilon_2 \leq \sqrt{\rho\varepsilon_1}, \\ \dfrac{\alpha\sigma}{N\varepsilon_2^2}, & \text{if } \sqrt{\alpha}\varepsilon_2 > \sqrt{\rho\varepsilon_1}. \end{cases}$$

The next theorem presents the main contribution of the article, which establishes the ε_1–ε_2 uniform convergence error estimate.

Theorem 5.5. *Let $y(x)$ and $Y(x_i)$ be respectively the solutions of the problems (1.1)–(1.4), and (3.2)–(3.3). Then, for sufficiently large N, we have*

$$\|Y - y\| \leq \begin{cases} CN^{-1}\ln N, & \text{if } \sqrt{\alpha}\varepsilon_2 \leq \sqrt{\rho\varepsilon_1}, \\ CN^{-1}(\ln N)^2, & \text{if } \sqrt{\alpha}\varepsilon_2 > \sqrt{\rho\varepsilon_1}. \end{cases}$$

Proof. From the results of Lemmas 2.3, 5.1–5.3 and using the methods adopted in [15], it ensues that

$$e(x_i) \leq \begin{cases} CN^{-1}\ln N, & \sqrt{\alpha}\varepsilon_2 \leq \sqrt{\rho\varepsilon_1}, \\ CN^{-1}(\ln N)^2, & \sqrt{\alpha}\varepsilon_2 > \sqrt{\rho\varepsilon_1}, \end{cases} \quad \forall\, x_i \in \Omega^N. \tag{5.8}$$

To prove the error at the point of discontinuity $x_i = x_{N/2}$:
Consider the case $\sqrt{\alpha}\varepsilon_2 \le \sqrt{\rho\varepsilon_1}$. Define the discrete barrier function $\phi_*(x_i)$ to be the solution of

$$\begin{aligned}&\varepsilon_1\delta^2\phi_*(x_i) + \varepsilon_2\alpha^* D^*\phi_*(x_i) - \gamma\phi_*(x_i) = 0,\\ &\phi_*(x_0) = 0,\ \phi_*(x_{N/2}) = 1 \qquad \text{and} \qquad \phi_*(x_N) = 0.\end{aligned}$$

We can prove that

$$D^-\phi_*(x_i) \ge 0, \quad \text{for } 1 \le i \le N/2 - 1 \qquad \text{and} \qquad D^+\phi_*(x_i) \le 0, \quad \text{for } 1 \le i \le N/2 + 1.$$

Note that $\mathcal{L}^N\phi_*(x_i) \le 0$ for all $x_i \in \Omega^N$. Define the ancillary continuous functions $z_1(x)$, $z_2(x)$ by

$$\begin{aligned}&\varepsilon_1 z_1''(x) - \alpha^*\varepsilon_2 z_1'(x) - \gamma z_1(x) = 0, \quad z_1(0) = 0,\ z_1(x_{N/2}) = 1,\\ &\varepsilon_1 z_2''(x) + \alpha^*\varepsilon_2 z_2'(x) - \gamma z_2(x) = 0, \quad z_2(x_{N/2}) = 1,\ z_2(1) = 0.\end{aligned}$$

On solving the above equations we get

$$z_1(x) = e^{\eta(d-x)}\left(\frac{\sinh(\mu x)}{\sinh(\mu d)}\right), \qquad z_2(x) = e^{\eta(d-x)}\left(\frac{\sinh(\mu(1-x))}{\sinh(\mu(1-d))}\right),$$

where, $\eta = \dfrac{\alpha^*\varepsilon_2}{2\varepsilon_1}$ and $\mu = \dfrac{\sqrt{(\alpha^*\varepsilon_2)^2 + 4\varepsilon_1\gamma}}{2\varepsilon_1}$. Thus, we have

$$\begin{aligned}|D^- z_1(x_{N/2})| &= \frac{\sinh(\mu d) - e^{\eta h}\sinh(\mu(d-h))}{\overline{h}_3\sinh(\mu d)}\\ &= \left(\frac{1 - e^{-(\mu-\eta)\overline{h}_3}}{\overline{h}_3}\right)\left(\frac{1 - e^{-2\mu(d-h-3)}}{1 - e^{-2\mu d}}\right)\\ &\ge C\left(\frac{1 - e^{-(\mu-\eta)\overline{h}_3}}{\overline{h}_3}\right)\end{aligned}$$

and also

$$|D^+ z_2(x_{N/2})| \ge C\left(\frac{1 - e^{-(\mu-\eta)\overline{h}_4}}{\overline{h}_4}\right).$$

Hence

$$(D^+ z_2 - D^- z_1)(x_{N/2}) = -(|D^+ z_2(x_{N/2})| + D^- z_1(x_{N/2})) \le -\frac{C(1 - e^{-\beta})}{\sqrt{\varepsilon_1}\beta} \le -\frac{C}{\sqrt{\varepsilon_1}}$$

where $\beta = \dfrac{\alpha^*\overline{h}}{2\sqrt{\varepsilon_1}}$, $\overline{h} = \max\{\overline{h}_3, \overline{h}_4\}$. Since $\dfrac{1 - e^{-\beta}}{\beta}$ is a decreasing function of β. Following the methods from [2] on each of the intervals $[0, d]$ and $[d, 1]$, we have

$$\begin{aligned}&|\phi_*(x_i) - z_1(x_i)| \le C(N^{-1}\ln N)^2, \quad \text{for } i \le d,\\ &|\phi_*(x_i) - z_2(x_i)| \le C(N^{-1}\ln N)^2, \quad \text{for } i \ge d.\end{aligned}$$

At the point $x_{N/2} = d$,

$$\begin{aligned}\left(D^+\phi_* - D^-\phi_*\right)(x_{N/2}) &= \frac{\phi_*(x_{N/2} + \overline{h}_4) - 1}{\overline{h}_4} - \frac{\phi_*(x_{N/2} + \overline{h}_3) - 1}{\overline{h}_3}\\ &\le \left(D^+ z_2(x_{N/2}) - D^- z_1(x_{N/2})\right) \pm \frac{C(N^{-1}\ln N)^2}{min\{\overline{h}_3, \overline{h}_4\}}\\ \left(D^+\phi_* - D^-\phi_*\right)(x_{N/2}) &\le -C/\sqrt{\varepsilon_1}.\end{aligned}$$

Consider the barrier

$$\psi_1^{\pm}(x_i) = C_3 N^{-1}\ln N + C_4\frac{h}{\sqrt{\varepsilon_1}}\phi_*(x_i) \pm e(x_i), \quad \forall\, x_i \in \overline{\Omega}^N.$$

Now, $\psi_1^{\pm}(x_0) \geq 0$, $\psi_1^{\pm}(x_N) \geq 0$ and

$$\mathcal{L}^N \psi_1^{\pm}(x_i) \leq 0, \quad x_i \in \Omega^N, \quad (D^+ - D^-)\psi_1^{\pm}(x_{N/2}) \leq 0, \quad i = N/2.$$

Hence applying the discrete minimum principle, we get $\psi_1^{\pm}(x_i) \geq 0 \; \forall \; x_i \in \overline{\Omega}^N$. For sufficiently large N we derive

$$|(Y - y)(x_i)| \leq CN^{-1}(\ln N), \quad \text{if} \quad \sqrt{\alpha}\varepsilon_2 \leq \sqrt{\rho\varepsilon_1}. \tag{5.9}$$

In the second case when $\sqrt{\alpha}\varepsilon_2 > \sqrt{\rho\varepsilon_1}$ consider the discrete barrier function $\psi_2(x_i) = \psi(x_i) \pm e(x_i)$ defined in the interval $(d - \sigma_2, d + \sigma_3)$ where

$$\psi(x_i) = CN^{-1}(\ln N)^2 + \frac{CN^{-1}\varepsilon_2^2\sigma}{\varepsilon_1^2} \begin{cases} (x_i - d - \sigma_2), & x_i \in (d - \sigma_2, d], \\ (d + \sigma_3 - x_i), & x_i \in [d, d + \sigma_3). \end{cases}$$

It could be seen that $\psi_2(d - \sigma_3) > 0$, $\psi_2(d + \sigma_3) > 0$ and $\mathcal{L}^N\psi_2(x_i) < 0$, $D^+\psi_2(x_i) - D^-\psi_2(x_i) < 0$. Applying the discrete minimum principle to $\psi_2(x_i)$, we find that $\psi_2(x_i) \geq 0$. Hence

$$|(Y - y)(x_i)| \leq \frac{CN^{-1}\sigma^2\varepsilon_2^2}{\varepsilon_1^2} \leq CN^{-1}(\ln N)^2, \quad \text{for } x_i \in (d - \sigma_2, d + \sigma_3). \tag{5.10}$$

Therefore, by combining (5.9) and (5.10) we obtain the desired result. □

6. Examples

In order to show the applicability of the present method we have considered some problems of singularly perturbed two parameter BVP with discontinuous convection coefficient and source term.

Example 6.1.

$$\varepsilon_1 y''(x) + \varepsilon_2 a(x) y'(x) - y(x) = f(x), \quad x \in (\Omega^- \cup \Omega^+),$$
$$y(0) = 2, \quad y(1) = 1,$$

with

$$a(x) = \begin{cases} -2, & 0 \leq x \leq 0.5 \\ 2, & 0.5 < x \leq 1, \end{cases} \quad \text{and} \quad f(x) = \begin{cases} -1, & 0 \leq x \leq 0.5 \\ 1, & 0.5 < x \leq 1. \end{cases}$$

Example 6.2.

$$\varepsilon_1 y''(x) + \varepsilon_2 a(x) y'(x) - 2y(x) = f(x), \quad x \in (\Omega^- \cup \Omega^+),$$
$$y(0) = 0, \quad y(1) = -1,$$

with

$$a(x) = \begin{cases} -(1 + x), & 0 \leq x \leq 0.5, \\ (2 + x^2), & 0.5 < x \leq 1, \end{cases} \quad \text{and} \quad f(x) = \begin{cases} -(14x + 1), & 0 \leq x \leq 0.5 \\ 2 - 2x, & 0.5 < x \leq 1. \end{cases}$$

The nodal errors are estimated using the double mesh principle stated by Doolan (see [1], page 199). Define the maximum point-wise error in the double mesh differences to be

$$E^N_{(\varepsilon_1,\varepsilon_2)} = \max_{x_i \in \overline{\Omega}^N} |Y^N(x_i) - Y^{2N}(x_i)|, \quad \text{and} \quad E^N = \max_{\varepsilon_1,\varepsilon_2} E^N_{(\varepsilon_1,\varepsilon_2)},$$

where $Y^N(x_i)$ and $Y^{2N}(x_i)$ represent the numerical solutions determined using N and $2N$ mesh intervals. The order of convergence is approximated using the ratio

$$R^N = \log_2\left(\frac{E^N}{E^{2N}}\right).$$

Tables 1 and 2 display the maximum point-wise errors for Example 6.1, varying ε_1 on the set $G_{\varepsilon_1} = \{10^{-0}, 10^{-2}, \ldots, 10^{-12}\}$, with $\varepsilon_2 = 10^{-3}$ and $\varepsilon_2 = 10^{-4}$, respectively. The maximum of the point-wise errors E^N are represented and the approximate orders of convergence R^N are presented in the last row of each table, showing almost order one which coincides with the theoretical results in 5.5.

Fig. 1a shows the numerical solution plots and Fig. 1b represents the numerical error plots for Example 6.1 for the displayed values. These two graphs correspond to the case when $\sqrt{\alpha}\varepsilon_2 < \sqrt{\rho\varepsilon_1}$.

Fig. 2a shows the numerical solution plots and Fig. 2b represents the numerical error plots for Example 6.1 for the displayed values. These two graphs correspond to the case when $\sqrt{\alpha}\varepsilon_2 > \sqrt{\rho\varepsilon_1}$.

Table 1
Maximum point-wise errors E^N and approximate orders of convergence R^N for Example 6.1 when $\varepsilon_2 = 10^{-3}$.

	Number of mesh points N				
ε_1	32	64	128	256	512
10^0	1.72000E−06	5.50370E−07	1.97780E−07	7.94860E−08	3.48920E−08
10^{-2}	2.03520E−03	6.56460E−04	2.36860E−04	9.54490E−05	4.19620E−05
10^{-4}	4.64330E−02	2.81190E−02	1.42360E−02	7.48330E−03	3.93490E−03
10^{-6}	1.34110E−01	1.00460E−01	6.51100E−02	4.02480E−02	2.36900E−02
10^{-8}	1.77540E−01	1.34610E−01	8.94960E−02	5.57030E−02	3.29910E−02
10^{-10}	1.78310E−01	1.35210E−01	8.99240E−02	5.59720E−02	3.31510E−02
10^{-12}	1.78310E−01	1.35220E−01	8.99290E−02	5.59740E−02	3.31530E−02
E^N	1.78310E−01	1.35220E−01	8.99290E−02	5.59740E−02	3.31530E−02
R^N	0.39916	0.58841	0.68402	0.75563	0.79931

Table 2
Maximum point-wise errors E^N and approximate orders of convergence R^N for Example 6.1 when $\varepsilon_2 = 10^{-4}$.

	Number of mesh points N				
ε_1	32	64	128	256	512
10^0	1.28800E−06	3.34170E−07	8.95750E−08	2.53770E−08	7.83640E−09
10^{-2}	1.53240E−03	3.99980E−04	1.07500E−04	3.04710E−05	9.41350E−06
10^{-4}	3.32830E−02	1.64650E−02	6.26380E−03	2.39580E−03	9.19960E−04
10^{-6}	4.63970E−02	2.81180E−02	1.42360E−02	7.48330E−03	3.93490E−03
10^{-8}	1.33790E−01	1.00400E−01	6.50950E−02	4.02450E−02	2.36890E−02
10^{-10}	1.76880E−01	1.34420E−01	8.94320E−02	5.56880E−02	3.29870E−02
10^{-12}	1.77630E−01	1.35020E−01	8.98590E−02	5.59550E−02	3.31470E−02
E^N	1.77630E−01	1.35020E−01	8.98590E−02	5.59550E−02	3.31470E−02
R^N	0.39573	0.58742	0.68339	0.7554	0.79921

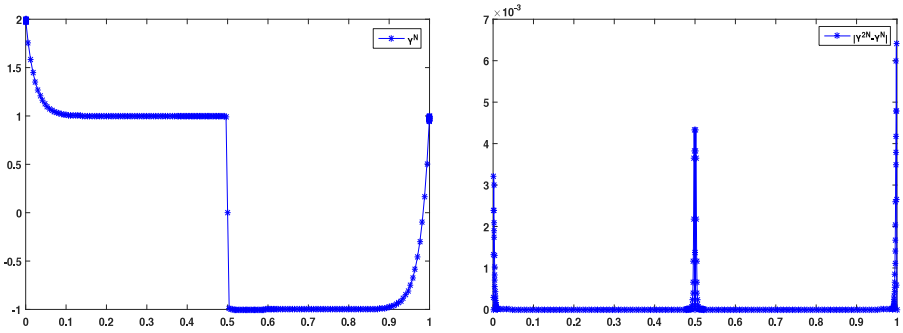

(a) Numerical Solution (b) Error = $|Y^{2N}(x_i) - Y^N(x_i)|$

Fig. 1. 1a & 1b: plots of numerical solution and errors for $\varepsilon_1 = 10^{-6}$, $\varepsilon_2 = 10^{-2}$ when $N = 256$ for Example 6.1.

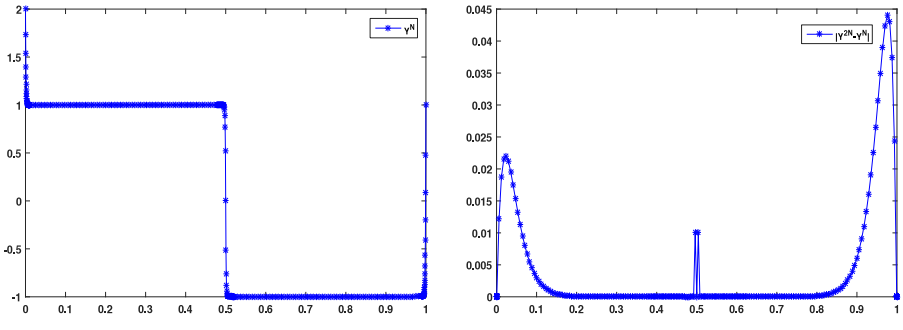

(a) Numerical Solution (b) Error = $|Y^{2N}(x_i) - Y^N(x_i)|$

Fig. 2. 2a & 2b: plots of numerical solution and errors for $\varepsilon_1 = 10^{-6}$, $\varepsilon_2 = 10^{-4}$ when $N = 256$ for Example 6.1.

Table 3
Maximum point-wise errors E^N and approximate orders of convergence R^N for Example 6.1 when $\varepsilon_1 = 10^{-5}$.

	Number of mesh points N				
ε_2	64	128	256	512	1024
10^0	1.107e−03	5.533e−04	2.765e−04	1.383e−05	6.912e−05
10^{-2}	1.977e−03	9.750e−04	4.841e−04	2.412e−05	1.204e−05
10^{-4}	2.706e−03	7.783e−04	2.439e−04	9.645e−05	4.439e−05
10^{-6}	1.162e−02	5.514e−02	3.057e−02	1.726e−03	9.681e−04
10^{-8}	2.712e−02	1.922e−02	1.229e−02	7.355e−03	4.219e−03
10^{-10}	4.523e−02	2.922e−02	1.831e−02	1.115e−02	6.488e−03
10^{-12}	5.729e−02	3.720e−02	2.284e−02	1.339e−02	7.602e−03
10^{-14}	5.814e−02	3.777e−02	2.325e−02	1.364e−02	7.746e−03
10^{-16}	5.818e−02	3.779e−02	2.327e−02	1.365e−02	7.753e−03
10^{-18}	5.820e−02	3.780e−02	2.327e−02	1.366e−02	7.755e−03
10^{-20}	5.820e−02	3.780e−02	2.327e−02	1.366e−02	7.756e−03
E^N	5.820e−02	3.780e−02	2.327e−02	1.366e−02	7.756e−03
R^N	0.62263	0.69992	0.768517	0.81657	0.84729

Table 4
Maximum point-wise errors E^N and approximate orders of convergence R^N for Example 6.2 when $\varepsilon_2 = 10^{-3}$.

	Number of mesh points N				
ε_1	32	64	128	256	512
10^0	2.20620E−03	1.64560E−03	8.34430E−04	4.73040E−04	2.14240E−04
10^{-2}	8.28080E−03	5.62030E−03	3.41650E−03	1.87990E−03	1.06910E−03
10^{-4}	1.86090E−02	1.47120E−02	1.04900E−02	6.67980E−03	3.92890E−03
10^{-6}	1.89710E−02	1.52030E−02	1.08760E−02	7.00130E−03	4.12160E−03
10^{-8}	1.89750E−02	1.52080E−02	1.08800E−02	7.00470E−03	4.12370E−03
10^{-10}	1.89750E−02	1.52080E−02	1.08810E−02	7.00470E−03	4.12370E−03
10^{-12}	1.89750E−02	1.52080E−02	1.08810E−02	7.00470E−03	4.12370E−03
E^N	1.89750E−02	1.52080E−02	1.08810E−02	7.00470E−03	4.12370E−03
R^N	0.319243789	0.483097342	0.635351041	0.764392856	0.820314554

Table 5
Maximum point-wise errors E^N and approximate orders of convergence R^N for Example 6.2 when $\varepsilon_2 = 10^{-4}$.

	Number of mesh points N				
ε_1	32	64	128	256	512
10^0	2.16490E−03	1.51470E−03	7.48460E−04	3.12630E−04	1.27810E−04
10^{-2}	2.20600E−03	1.64820E−03	8.35460E−04	4.74140E−04	2.14480E−04
10^{-4}	8.32360E−03	5.65050E−03	3.43600E−03	1.89040E−03	1.07530E−03
10^{-6}	1.87170E−02	1.48000E−02	1.05530E−02	6.72070E−03	3.95290E−03
10^{-8}	1.90810E−02	1.52950E−02	1.09420E−02	7.04410E−03	4.14680E−03
10^{-10}	1.90850E−02	1.53000E−02	1.09470E−02	7.04750E−03	4.14880E−03
10^{-12}	1.90850E−02	1.53000E−02	1.09470E−02	7.04750E−03	4.14890E−03
E^N	1.90850E−02	1.53000E−02	1.09470E−02	7.04750E−03	4.14890E−03
R^N	0.318914630	0.483043762	0.635285690	0.764405660	0.820311523

Table 3 displays the maximum point-wise errors for Example 6.1, varying ε_2 on the set $G_{\varepsilon_2} = \{10^{-0}, 10^{-2}, \ldots, 10^{-20}\}$ with $\varepsilon_1 = 10^{-5}$. The maximum pointwise error E^N is represented and the approximate orders of convergence R^N are calculated in the last row of each table, showing almost order one, which coincides with the theoretical results in 5.5.

Tables 4 and 5 display the maximum point-wise errors for Example 6.2 with $\varepsilon_2 = 10^{-3}$ and $\varepsilon_2 = 10^{-4}$ respectively for different values of $\varepsilon_1 \in G_{\varepsilon_1}$. The orders of convergence (R^N) is included in the last row of the tables, which shows almost order one.

Table 6 displays the maximum point-wise errors for Example 6.2, varying ε_2 on G_{ε_2} with $\varepsilon_1 = 10^{-7}$. The maximum point-wise errors E^N are represented and the orders of convergence R^N are calculated in the last row of each table, showing almost order one which coincides with the theoretical results in 5.5.

Fig. 3a represents the numerical solution plots and Fig. 3b represents the numerical error plots for Example 6.2 for the displayed values. These two graphs correspond to the case when $\sqrt{\alpha}\varepsilon_2 < \sqrt{\rho\varepsilon_1}$.

Table 6
Maximum point-wise errors E^N and approximate orders of convergence R^N for Example 6.2 when $\varepsilon_1 = 10^{-7}$.

	Number of mesh points N				
ε_2	64	128	256	512	1024
10^{0}	2.460e−04	1.218e−04	6.061e−05	3.023e−05	1.510e−05
10^{-2}	4.386e−03	2.172e−03	1.081e−03	5.390e−04	2.692e−04
10^{-4}	7.031e−03	3.164e−03	1.509e−03	7.391e−04	3.662e−04
10^{-6}	3.482e−02	1.183e−02	4.165e−03	1.612e−03	7.060e−04
10^{-8}	1.060e−01	6.447e−02	4.647e−02	2.993e−02	1.814e−02
10^{-10}	2.052e−01	1.878e−01	1.468e−01	1.008e−02	6.308e−02
10^{-12}	2.323e−01	1.568e−01	9.992e−01	5.977e−02	3.444e−02
10^{-14}	2.416e−01	1.631e−01	1.047e−01	6.335e−02	3.657e−02
10^{-16}	2.421e−01	1.635e−01	1.050e−01	6.354e−02	3.668e−02
10^{-18}	2.422e−01	1.636e−01	1.051e−01	6.360e−02	3.672e−02
10^{-20}	2.422e−01	1.636e−01	1.051e−01	6.360e−02	3.672e−02
E^N	2.422e−01	1.636e−01	1.051e−01	6.360e−02	3.672e−02
R^N	0.5660	0.6384	0.7246	0.7924	0.8346

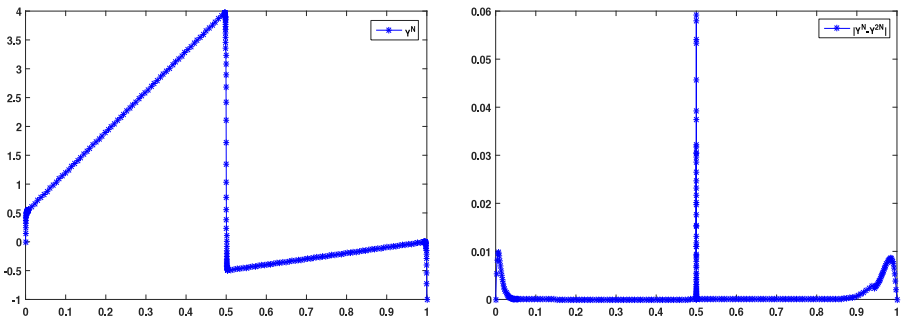

(a) Numerical Solution (b) Error = $|Y^{2N}(x_i) - Y^N(x_i)|$

Fig. 3. 3a & 3b: plots of numerical solution and errors for $\varepsilon_1 = 10^{-6}$, $\varepsilon_2 = 10^{-2}$ when $N = 256$ for Example 6.2.

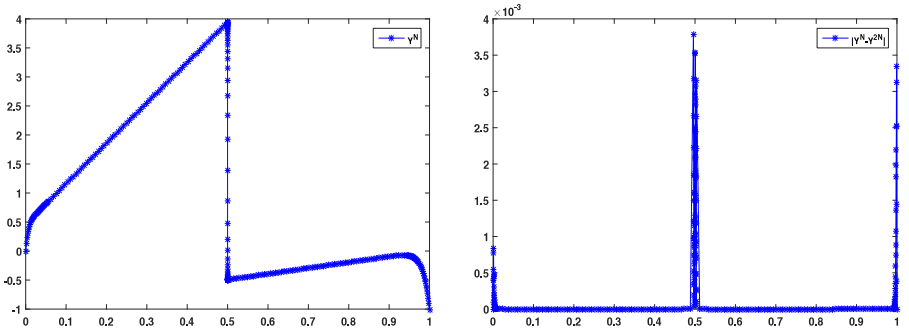

(a) Numerical Solution (b) Error = $|Y^{2N}(x_i) - Y^N(x_i)|$

Fig. 4. 4a & 4b: plots of numerical solution and errors for $\varepsilon_1 = 10^{-6}$, $\varepsilon_2 = 10^{-4}$ when $N = 256$ for Example 6.2.

Fig. 4a represents the numerical solution plots and Fig. 4b represents the numerical error plots for Example 6.2 for the displayed values. These two graphs correspond to the case when $\sqrt{\alpha}\varepsilon_2 > \sqrt{\rho\varepsilon_1}$.

7. Conclusion

A numerical method is discussed to solve reaction–convection–diffusion singularly perturbed second order ordinary differential equation having two small parameters with discontinuity at the convection coefficient and source term. This technique is based on upwind finite difference scheme with piecewise uniform Shishkin mesh. The method is shown to be uniformly convergent and independent of the mesh parameters and perturbation parameters with almost first order

convergence. Error bounds for the numerical scheme are derived. Some numerical examples are presented to illustrate the parameter-uniform convergence of the numerical approximations.

Acknowledgments

The authors are grateful to the referees for several constructive comments and remarks.

References

[1] E.P. Doolan, J.J.H. Miller, W.H. Schilders, Uniform Numerical Methods for Problems with Initial and Boundary Layers, volume 1, Boole Press, 1980.
[2] P.A. Farrell, A. Hegarty, J.J.H. Miller, E. O'Riordan, G.I. Shishkin, Robust Computational Techniques for Boundary Layers, CRC Press, 2000.
[3] H.G. Roos, M. Stynes, L. Tobiska, Robust Numerical Methods for Singularly Perturbed Differential Equations: Convection-Diffusion-Reaction and Flow Problems, volume 24, Springer Science & Business Media, 2008.
[4] S. Natesan, J. Vigo-Aguiar, N. Ramanujam, A numerical algorithm for singular perturbation problems exhibiting weak boundary layers, Comput. Math. Appl. 45 (1–3) (2003) 469–479.
[5] J. Vigo-Aguiar, S. Natesan, An efficient numerical method for singular perturbation problems, J. Comput. Appl. Math. 192 (1) (2006) 132–141.
[6] M. Chandru, T. Prabha, V. Shanthi, A hybrid difference scheme for a second-order singularly perturbed reaction-diffusion problem with non-smooth data, Int. J. Appl. Comput. Math. 1 (1) (2015) 87–100.
[7] M. Chandru, V. Shanthi, Fitted mesh method for singularly perturbed robin type boundary value problem with discontinuous source term, Int. J. Appl. Comput. Math. 1 (3) (2015) 491–501.
[8] P. Farrell, J. Miller, E. O'Riordan, G. Shishkin, Singularly perturbed differential equations with discontinuous source terms, in: Proceedings of Analytical and Numerical Methods for Convection-Dominated and Singularly Perturbed Problems, Lozenetz, Bulgaria, 1998, pp. 23–32.
[9] P.A. Farrell, A.F. Hegarty, J.J.H. Miller, E. O'Riordan, G.I. Shishkin, Singularly perturbed convection–diffusion problems with boundary and weak interior layers, J. Comput. Appl. Math. 166 (1) (2004) 133–151.
[10] R.E. O'Malley, Two-parameter singular perturbation problems for second-order equations (constant and variable coefficient initial and boundary value problems for second order differential equations), J. Appl. Math. Mech. 16 (1967) 1143–1164.
[11] J. Vigo-Aguiar, S. Natesan, A parallel boundary value technique for singularly perturbed two-point boundary value problems, J. Supercomput. 27 (2) (2004) 195–206.
[12] H.G. Roos, Z. Uzelac, The SDFEM for a convection-diffusion problem with two small parameters, Comput. Methods Appl. Math. 3 (3) (2003) 443–458.
[13] K.C. Patidar, A robust fitted operator finite difference method for a two-parameter singular perturbation problem, J. Difference Equ. Appl. 14 (12) (2008) 1197–1214.
[14] G. Shishkin, V. Titov, A difference scheme for a differential equation with two small parameters at the derivatives, Chisl. Metody Meh. Sploshn. Sredy 7 (2) (1976) 145–155.
[15] E. O'Riordan, M.L. Pickett, G.I. Shishkin, Singularly perturbed problems modeling reaction-convection-diffusion processes, Comput. Methods Appl. Math. 3 (3) (2003) 424–442.
[16] V. Shanthi, N. Ramanujam, S. Natesan, Fitted mesh method for singularly perturbed reaction-convection-diffusion problems with boundary and interior layers, J. Appl. Math. Comput. 22 (1–2) (2006) 49–65.
[17] M. Chandru, T. Prabha, V. Shanthi, A parameter robust higher order numerical method for singularly perturbed two parameter problems with non-smooth data, J. Comput. Appl. Math. 309 (2017) 11–27.
[18] C. De Falco, E. O'Riordan, Interior layers in a reaction diffusion equation with a discontinuous diffusion coefficient, Int. J. Numer. Anal. Model. 7 (3) (2010) 444–461.
[19] P.A. Farrell, A.F. Hegarty, J.J. Miller, E. O'Riordan, G.I. Shishkin, Global maximum norm parameter-uniform numerical method for a singularly perturbed convection-diffusion problem with discontinuous convection coefficient, Math. Comput. Modelling 40 (11–12) (2004) 1375–1392.